Experimental Eye Research 220 (2022) 109103

Contents lists available at ScienceDirect

Experimental Eye Research

journal homepage: www.elsevier.com/locate/yexer

Research article

Measurement of postmortem outflow facility using *iPerfusion*

Michael Madekurozwa, Ester Reina-Torres, Darryl R. Overby **, Joseph van Batenburg-Sherwood *

Dept. of Bioengineering, Imperial College London, London, SW7 2AZ, UK

ARTICLE INFO

Keywords:
Mouse models
Perfusion
Outflow facility
Postmortem effects

ABSTRACT

The key risk factor for glaucoma is elevation of intraocular pressure (IOP) and alleviating it is the only effective therapeutic approach to inhibit further vision loss. IOP is regulated by the flow of aqueous humour across resistive tissues, and a reduction in outflow facility, is responsible for the IOP elevation in glaucoma. Measurement of outflow facility is therefore important when investigating the pathophysiology of glaucoma and testing candidate treatments for lowering IOP. Due to similar anatomy and response to pharmacological treatments, mouse eyes are a common model of human aqueous humour dynamics. The *ex vivo* preparation, in which an enucleated mouse eye is mounted in a temperature controlled bath and cannulated, has been well characterised and is widely used. The postmortem *in situ* model, in which the eyes are perfused within the cadaver, has received relatively little attention. In this study, we investigate the postmortem *in situ* model using the *iPerfusion* system, with a particular focus on i) the presence or absence of pressure-independent flow, ii) the effect of evaporation on measured flow rates and iii) the magnitude and pressure dependence of outflow facility and how these properties are affected by postmortem changes. Measurements immediately after cannulation and following multi-pressure facility measurement demonstrated negligible pressure-independent flow in postmortem eyes, in contrast to assumptions made in previous studies. Using a humidity chamber, we investigated whether the humidity of the surrounding air would influence measured flow rates. We found that at room levels of humidity, evaporation of saline droplets on the eye resulted in artefactual flow rates with a magnitude comparable to outflow, which were eliminated by a high relative humidity (>85%) environment. Average postmortem outflow facility was ~4 nl/min/mmHg, similar to values observed *ex vivo*, irrespective of whether a postmortem delay was introduced prior to cannulation. The intra-animal variability of measured outflow facility values was also reduced relative to previous *ex vivo* data. The pressure-dependence of outflow facility was reduced in the postmortem relative to *ex vivo* model, and practically eliminated when eyes were cannulated >40 min after euthanisation. Overall, our results indicate that the moderately increased technical complexity associated with postmortem perfusion provides reduced variability and reduced pressure-dependence in outflow facility, when experimental conditions are properly controlled.

1. Introduction

Glaucoma is a world leading cause of irreversible blindness (Quigley and Broman, 2006), the only effective therapeutic target for which is lowering intraocular pressure (IOP) (Leske et al., 2003; Morrison et al., 1998; Heijl et al., 2002). IOP is determined by aqueous humour dynamics (AHD), as described by Goldmann's equation:

$$P = \frac{Q_{perf} + Q_{in} - Q_u}{C} + P_{ev} \quad (1)$$

where P is the intraocular pressure, Q_{in} is inflow, Q_u is the pressure-independent outflow, C is the total outflow facility[1] and P_{ev} is

* Corresponding author.
** Corresponding author.
E-mail addresses: d.overby@imperial.ac.uk (D.R. Overby), jvbsherwood@imperial.ac.uk (J. van Batenburg-Sherwood).

[1] The total outflow facility C consists of conventional outflow facility and pressure-dependent components of unconventional outflow, as well as pseudo-facility (pressure-dependent changes in aqueous humour secretion), which applies *in vivo*. In the present study, as all eyes were perfused postmortem, there is zero pseudo-facility, and so for simplicity we refer to C as the 'outflow facility'. Note that it is not possible to discern anatomical outflow pathways, namely conventional vs unconventional, by perfusion alone. However, in postmortem or enucleated eyes, conventional outflow is expected to be the main contributor to C.

https://doi.org/10.1016/j.exer.2022.109103
Received 20 January 2022; Received in revised form 24 April 2022; Accepted 28 April 2022
Available online 5 May 2022
0014-4835/© 2022 The Authors. Published by Elsevier Ltd. This is an open access article under the CC BY license (http://creativecommons.org/licenses/by/4.0/).

episcleral venous pressure. Q_{perf} is additional flow into the eye from a perfusion system during experimentation. The primary cause of elevated IOP is a decrease in outflow facility (Kwon et al., 2009; Grant, 1951; Stamer and Acott, 2012), and hence it is important to have models and tools capable of accurately measuring C in order to investigate its regulation and dysregulation.

Mice are a common model for the study of AHD, as their anatomy and physiology resemble that of humans (Smith, 2002; Overby et al., 2014). Furthermore, they exhibit a comparable pharmacological response to a number of drugs that affect outflow facility (Whitlock et al., 2010; Boussommier-Calleja et al., 2012; Crowston et al., 2004; Akaishi et al., 2009). In mice, outflow facility is typically calculated from measurements of the flow-pressure relationship obtained via the perfusion of eyes in living animals (*in vivo*) (e.g. Ko et al., 2016; Camras et al., 2010; Millar et al., 2011; Aihara et al., 2003; Yelenskiy et al., 2017; Yu et al., 2020, Roy Chowdhury et al., 2017), in *in situ* eyes following death (herein 'postmortem') (e.g. Millar et al., 2011; Aihara et al., 2002), or following enucleation (herein *ex vivo*) (e.g. Boussommier-Calleja et al., 2012; Boussommier-Calleja et al., 2015; Boussommier-Calleja and Overby, 2013; Lei et al., 2011, Kizhatil et al., 2016, Reina-Torres et al., 2019; Madekurozwa et al., 2021, Roy Chowdhury et al., 2017). *Ex vivo* and postmortem eyes offer a simpler approach because elimination of inflow and episcleral venous pressure following death removes what would otherwise be significant uncertainties that affect the calculation of C.

We recently demonstrated that previous approaches to analysing *ex vivo* pressure and flow data can lead to errors of up to several hundred percent (Sherwood et al., 2016; Madekurozwa et al., 2017). The established approach assumes a constant (pressure-independent) C, that is taken as the slope of a straight line fit to flow-pressure data. The intercept represents an extrapolated estimate of the pressure-independent outflow and has typically been interpreted as unconventional or uveoscleral outflow. By using an open-loop pressure approach (rather than a syringe pump based method), *iPerfusion* allows measurement of the flow rate at zero-pressure, thereby allowing direct-measurement of pressure-independent outflow. We demonstrated that for *ex vivo* eyes, there is no pressure-independent outflow (Sherwood et al., 2016), and that when we imposed an artificial pressure-independent flow using a syringe pump via a second cannula, we were able to accurately measure this imposed flow (Madekurozwa et al., 2017). We then demonstrated that outflow facility in *ex vivo* mouse eyes is pressure-dependent, increasing with pressure, likely due to anterior chamber (AC) deepening and/or insufficient hydration of the eye during perfusion (Sherwood et al., 2016; Madekurozwa et al., 2017, Boussommier-Calleja et al., 2015, Grant, 1963). We proposed a power-law model (Sherwood et al., 2016) that accounts for the pressure-dependence of outflow facility and has since been used in numerous studies (e.g. Bertrand et al. (2020), Li et al. (2019), Li et al. (2020), Reina-Torres et al. (2017)).

The magnitude of pressure-independent flow and suitability of a power-law fit have not yet been evaluated in the postmortem or cadaveric (i.e., non-enucleated) eye. Furthermore, as compared with the *ex vivo* model, the postmortem eye retains connection to the native distal vasculature through which aqueous humour eventually leaves the eye and avoids potential artefacts caused during enucleation. It does, however, introduce potential effects due to time-dependent postmortem changes, such as the onset of rigor mortis, and technical challenges to ensure sufficient hydration of the eye.

Therefore, it seems pertinent to properly characterise the flow-pressure relationship and outflow facility in the postmortem cadaveric eye. Specifically, we address the following questions in postmortem C57BL/6J mouse eyes:

1) What is the magnitude of pressure-independent flow (Q_0[2]) at the start of a perfusion and does it change over time?
2) Is the magnitude of pressure-independent flow Q_0 altered by evaporative losses from the surface of the eye?
3) What is the magnitude of outflow facility, does facility exhibit a pressure-dependence or non-linearity, and does the time between death and perfusion affect the measured facility?

Lastly, we address an important retrospective question:

4) How does outflow facility measured in postmortem eyes compare to that previously reported in *ex vivo* eyes using *iPerfusion*?

2. Material and methods

2.1. Experimental design

Multiple groups of mice were used to address the above questions. An overview of the experimental groups is summarised in Table 1. A fourth group of 43 previously reported eyes perfused *ex vivo* during the same time period as the eyes included in the current study and following similar protocols (Reina-Torres et al., 2019; Reina-Torres et al., 2020a) was used to address Question 4.

To determine the magnitude of the pressure-independent flow (Question 1), we measured Q_0 directly after acclimatisation (~75 min after death, Group 1) and after acclimatisation and multi-pressure perfusion (~190 min after death, Group 2). The effect of evaporative losses (Question 2) was evaluated in Group 2, in which the relative humidity (RH) was controlled using a custom humidity chamber, and net pressure-independent outflow (Q_0) values were compared between high and room level RH values. The magnitude and non-linearity of outflow facility (Question 3) were assessed in Groups 2 and 3, where eyes underwent a multi-pressure perfusion protocol. The effect of time between death and perfusion on the measured facility was addressed by comparing Group 2 to Group 3, in which the time between death and cannulation was reduced from 40 min to less than 15 min, respectively.

Table 1
Overview of the three groups of mice used for postmortem experiments, along with their purpose and brief experimental protocols. Acclimatisation was 30 min at 8 mmHg for all cases. Repositioning of the cannula was not necessary in Group 2.

Group 1	Group 2	Group 3
N = 5 eyes from 5 animals	N = 10 eyes from 5 animals	N = 12 eyes from 6 animals
Question 1	Questions 2-4	Questions 3 and 4
1 Cannulate within 15 min of euthanisation	1 Cannulate >40 min after euthanisation	1 Cannulate within 15 min of euthanisation
2 Acclimatise	2 Acclimatise	2 Acclimatise
3 Reposition cannula	3 Measure outflow facility	3 Reposition cannula
4 Measure Q_0 at 0 mmHg	4 Measure Q_0 at 0 mmHg	4 Measure outflow facility
	5 Investigate effect of humidity on Q_0 at 0 mmHg in N = 4 eyes	

[2] We use the term Q_0 to represent the net pressure-independent flow, defined as the difference between inflow (Q_{in}) and pressure-independent outflow (Q_u), according to $Q_0 = Q_{in}$-Q_u (Madekurozwa et al., 2017). In *ex vivo* and postmortem eyes, $Q_{in} = 0$, hence Q_0 reflects total pressure-independent outflow.

2.2. Detailed methods

2.2.1. Animal Husbandry

Male C57BL/6J mice (Charles River Ltd, UK) aged 10–14 weeks were housed in individually ventilated enclosures at 21 °C with a 12 h light-dark cycle (lights on at 7AM). Food and water were supplied *ad libitum*. To prevent coagulation, 0.3 ml of heparin (6 mg/ml in PBS, Sigma-Aldrich, DE) was administered via intraperitoneal (IP) injection. Five minutes after heparin administration, mice were euthanised by IP administration of 150 mg/kg of pentobarbital (Pentoject; Animalcare, UK), with confirmation of death provided by the severing of the left femoral vein and artery. All experiments were performed in compliance with the ARVO Statement for the Use of Animals in Ophthalmic and Vision Research under the authority of a UK Home Office Project License.

2.2.2. Ocular perfusion setup

The cadaver was placed on a custom-built heat mat set to 35 °C and a rectal temperature probe (RET-3; WPI, USA) was inserted. The head was firmly held in place by a palate bar assembly (Model 933-B; KOPF, USA). Dulbecco's phosphate buffered saline (PBS) containing calcium and magnesium and supplemented with 5.5 mM glucose (DBG) was passed through a sterile 0.22 μm filter. Prior to perfusion, a drop of DBG was placed on the cornea of each eye, thereby ensuring that the external fluid on the corneal surface was isosmotic with the perfusate in the AC to prevent osmotically driven flow across the cornea, which would appear as a pressure-independent flow measured during perfusion. The cadaver was placed in a custom-built humidity chamber set to maintain the RH >85%, monitored with an environmental sensor (SHT2X/7X; Sensirion, Switzerland). The humidity chamber was made by coupling a household humidifier to a chamber made from aluminium struts and clear acrylic.

Prior to cannulation, the pressure readings were referenced to the height of the drop of DBG on the corneal surface (P_{drop}). The eyes were AC cannulated under a dissection microscope. A wire loop was used to proptose the eye by applying gentle pressure to the inferior eye lid. Using the wire loop to support the eye, a glass needle was then advanced into the anterior chamber (Fig. 1b). A video of the cannulation procedure is provided as Supplemental Information. The cannulation needles were fabricated as previously described (Madekurozwa et al., 2017) with a tip outer diameter of approximately 70 μm, a bevel angle of 45° and a hydraulic resistance of <0.5 mmHg/(μl/min). See the Supplemental Information for additional details.

iPerfusion (Sherwood et al., 2016) was used for perfusion measurements. Briefly, *iPerfusion* comprises an actuated pressure reservoir that controls the pressure applied to the eye (P_a), a thermal flow sensor (SLG150; Sensirion AG, Switzerland) for the measurement of the flow rate from the system into the eye (Q) and a pressure transducer (PX409; Omegadyne, USA) that measures the pressure within the eye (P) relative to P_{drop} (Fig. 1a). Acquired flow and pressure data were filtered with a 1st order Savitzky-Golay filter with a 60 s window length.

2.2.3. Pressure-independent flow experiments (Group 1)

For Group 1, one randomly selected eye from each mouse (N = 5) were AC cannulated within 15 min of death and set to acclimatise at 8 mmHg for 30 min, after which the needle was repositioned to minimise tension on the cornea. A direct measurement of the pressure-independent flow in the eye was obtained by setting the applied pressure to 0 mmHg (i.e. $P_a = P_{drop}$) after the acclimatisation period, as described previously (Madekurozwa et al., 2017). As the pressure in the eye approached 0 mmHg (P→0) the flow rate Q(P→0) was measured over a 30 min period. The last 5 min of the flow rate and pressure were taken to be steady state data and extracted for further analysis.

2.2.4. Outflow facility experiments (Group 2)

To ascertain the facility of postmortem eyes, Group 2 (N = 5 pairs) were perfused in five phases (Fig. 2).

Phase I: setup and cannulation. Within 15 min of death animals were placed on a bite bar and heat mat set to 35 °C at room RH. A postmortem delay of 40 min was allowed to pass, after which the eyes were AC cannulated.

Phase II: acclimatisation. Eyes were set to acclimatise at 8 mmHg for 30 min. During this phase, RH was raised from room level to >85% (Fig. 2a).

Phase III: measuring outflow facility. A multi-pressure perfusion was performed in which the pressure in the eye was varied from 5 to 17 mmHg in incremental steps of 1.5 mmHg, followed by a reduction down to 8 mmHg. Steady state for each step above 5 mmHg was defined when the rate of change of flow rate measured over a 5 min period was continuously below 5 nl/min/min for 60 s. The last 4 min of each pressure step were extracted, filtered, and defined as the steady state flow rate, Q, and pressure, P (Fig. 2b, blue highlighted regions). The mean and two standard deviations of the steady state regions are as presented by the data points and error bars in Fig. 2c. In order to estimate outflow facility, a power law model (which assumes that $Q_0 = 0$ nl/min) was fit to the steady state Q and P values, based on our previous study (Sherwood et al., 2016):

$$Q(P) = C_r\left(\frac{P}{P_r}\right)^{\beta} P \tag{2}$$

where C_r is a reference facility at a reference pressure of $P_r = 8$ mmHg, representing the approximate physiological pressure drop between the anterior chamber and episcleral vessels for C57BL/6J mice. The exponent β characterises the non-linearity of the flow-pressure relationship, or equivalently the pressure-dependence of outflow facility. A sample steady state Q-P plot with Eq. (2) fit to the data is shown in Fig. 2c.

Phase IV: total pressure-independent flow after a long-term perfusion. To

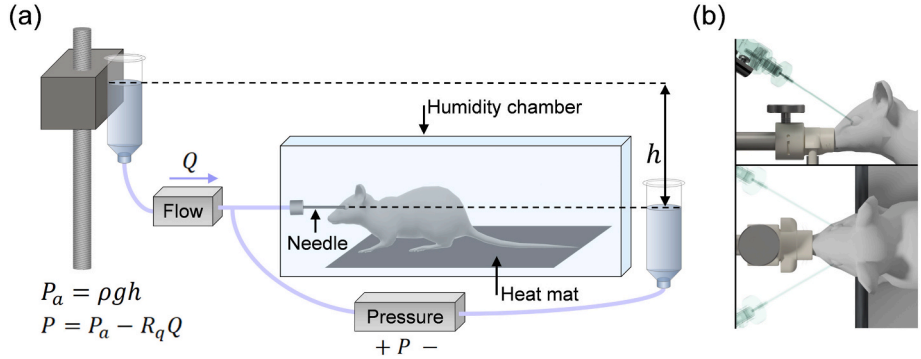

Fig. 1. Experimental setup for the perfusion of *in situ* eyes. a) *iPerfusion* system with the addition of a humidity chamber, heat mat and bite bar. P_a is the total pressure drop applied across the system, R_q is the hydrodynamic resistance of the flow sensor, ρ is the density of the perfusion fluid and *g* is the gravitational acceleration. b) Needle positions and use of a bite bar to restrain the head (also see Supplemental Information).

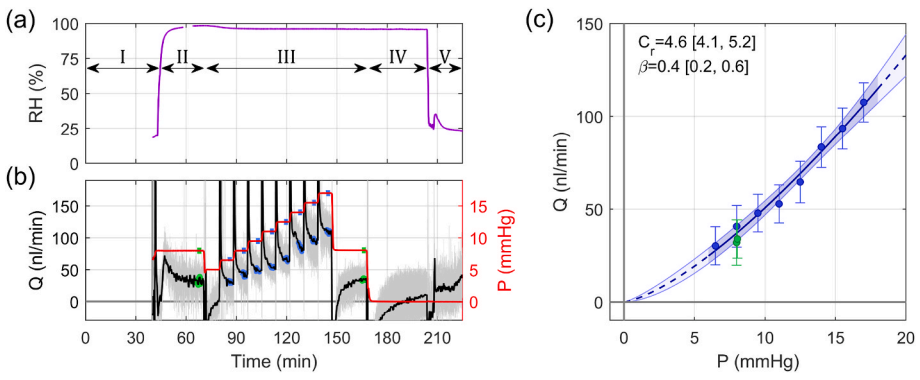

Fig. 2. Sample perfusion from the outflow facility experiments. a) Relative humidity in the enclosure. Experimental phases (I–V) are indicated as described in §2.2.4. b) Measured flow rate (Q) and pressure (P). Raw Q tracing is shown in grey, with the filtered Q and P signals shown in black and red respectively. Steady state Q and P readings used in the data analysis are highlighted in blue, with the values at the end of acclimatisation and post-perfusion at 8 mmHg shown in green. c) Q-P data from a single eye. Data points show the mean and two standard deviations of the steady state Q and P values (error bars on P are smaller than the symbols). The power law fit (Eq. (2)) to the steady state Q-P data is given by the blue curve with the 95% confidence interval (CI) of the fit shown as a shaded blue region. Dashed lines indicate extrapolated regions. Green data points (not used in the fit) demonstrate temporally stable outflow facility during the experiments, acquired during the acclimatisation and post-perfusion at 8 mmHg. (For interpretation of the references to colour in this figure legend, the reader is referred to the Web version of this article.)

investigate whether the magnitude of Q_0 changes after the multi-pressure perfusion (>160 min after death), pressure in the eyes was set to 0 mmHg and Q(P→0) was measured for 30 min at high RH as described in Section 2.2.3.

Phase V: effect of humidity on pressure-independent flow measurements. The effect of evaporation on apparent pressure-independent flow was measured by reducing the RH from >85% to room level (<65%), while measuring Q at P = 0 (P_a=P_{drop}) over a period of 30 min as described above. Throughout the procedure, the DBG drop was left undisturbed on the corneal surface. RH was decreased to room level by carefully opening the enclosure, drying the interior surface to remove condensation, closing the enclosure and exchanging air inside it (~70 l) with room air at ~50 l/min for 15 min. This procedure was successful in 4 eyes from 3 mice because retraction of the eyes during the postmortem delay caused dislodging of the needle in the 2 unsuccessful procedures.

2.2.5. *Effect of postmortem time on facility experiments (Group 3)*

Group 3 (N = 6 pairs of eyes) was used to investigate the effect of postmortem changes during the time between death and cannulation on outflow facility, by cannulating less than 15 min after death (in contrast to 40 min in Group 2). As in Group 2, the eyes were set to acclimatise at 8 mmHg for 30 min following cannulation, after which the needles were repositioned to minimise tension on the cornea. This was necessary due to retraction of the eye into the orbit. The pressure in the eyes was then varied from 5 mmHg to 23 mmHg in steps of 3 mmHg with the same pressure stepping criterion as Group 2.

2.3. *Statistics*

Data is reported in the form of X [lower CI, upper CI], where for normally distributed data such as flow rate, pressure and β, X represents the arithmetic mean. For log-normally distributed data such as facility (Sherwood et al., 2016, Reina-Torres et al., 2019), X represents the geometric mean. Normality and log-normality were evaluated using the Shapiro-Wilk test. Equal variances between groups were evaluated using Levene's test.

To avoid the deficiency in interpreting p-values, which can vary by orders of magnitude for different random samples from the same underlying populations (Cumming, 2014), we report 95% confidence intervals as our main indication of statistical uncertainty where relevant. We also provide p-values relative to a significance level of α = 0.05, but indicate where calculated p-values are less than 0.01 or 0.001.

For evaluation of P(P→0) and Q(P→0) (Section 3.1), we included data from one eye of each of the five mice from Group 1 and from both eyes from each of the five mice from Group 2. For statistical analysis, we averaged P(P→0) and Q(P→0) values for both eyes from Group 2 to yield 5 independent values. Normality was not rejected for either Group 1 or the averaged data from Group 2 ($p > 0.05$). For each group, we evaluated whether the arithmetic means of P(P→0) and Q(P→0) were different from zero using a two-tailed *t*-test.

In Section 3.3 we evaluate differences in facility, C_r, and nonlinearity, β, between Groups 2 and 3. Normality was not rejected for either group for β or log(C_r) ($p > 0.05$, the Shapiro-Wilk test) and the presence of equal variances was not rejected for either parameter ($p > 0.05$, Levene's test). In order to make use of both eyes from individual animals, the nested ANOVA analysis described by Rosner (1982) was used to compare differences in group means, with group as a fixed effect, and animal and eye (OS/OD) as random effects. The intraclass correlation coefficient (ICC, Rosner (1982)) was used to evaluate the relative independence of two eyes from the same animal in the present data set. To address whether the higher pressures used in Group 3 (up to 23 mmHg) influenced the statistical measurements, the analysis was repeated with only pressure steps in the range 5–17 mmHg.

The ICC for β (0.36) and C_r (0.26) indicated that there was no statistical correlation between two eyes from the same animal, and thus each eye can be treated as independent. Therefore, *t*-tests were used to evaluate whether the average value of β for all eyes from each group was statistically different from zero (Section 3.3).

For comparisons between Groups 2 and 3 with *ex vivo* data (Section 3.4), analyses were carried out under the assumption that eyes from the same animal were independent (due to low ICC as described in Section 3.3). In order to confirm that this did not introduce errors, the evaluation was also carried out conservatively with the average of both eyes from the same animal, which yielded the same conclusions. Although normality was not rejected for any of the groups, equality of variances was rejected ($p < 0.05$ for log(C_r) and $p < 0.01$ for β), hence the non-parametric Kruskall-Wallis test was applied. Post-hoc analyses were carried out using Dunn's test.

3. Results

3.1. *Postmortem pressure-independent flow*

To measure pressure-independent flow in Group 1, the applied pressure was set to 0 mmHg after acclimatisation. The resulting exponential decay of pressure and flow from one eye of 5 mice in Group 1 are shown in Fig. 3a, with the steady state P(P→0) and Q(P→0) values shown in Fig. 3b. The average pressure-independent flow across all 5 independent eyes was Q(P→0) = 0.7 [−4.2, 5.7] nl/min ($p > 0.05$, N = 5) with P(P→0) = 0.04 [−0.01, 0.09] mmHg ($p > 0.05$, N = 5). Equivalent data for 5 pairs of eyes following a long-term perfusion (Group 2) are shown in Fig. 3c and d. Averaging measurements between

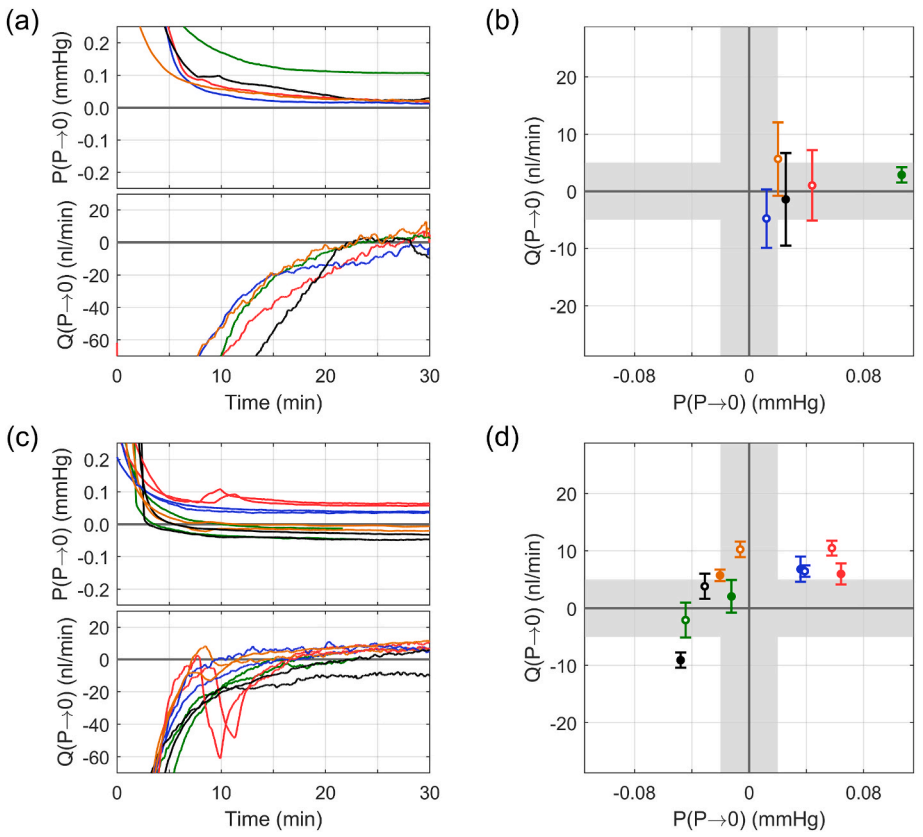

Fig. 3. Pressure-independent flow in a mouse cadaver from Group 1 (a, b) and Group 2 (c, d). a) and c) show the direct measurement of P(P→0) and Q (P→0) over a 30 min period which either began 45 min after the death of the animal (a) or at least 160 min after the death of the animal (c). The mean and two standard deviations on the last 5 min of data from the flow (Q) and pressure (P) measurements in panels a) and c) are shown as data points with error bars in panel b) and d) respectively (error bars in P are smaller than the symbols). In b) and d), the sensor uncertainty is indicated by the grey regions. In c) and d) eyes from the same cadaver are plotted in the same colour and measurements from OS are indicated by hollow points. OD and OS data for each cadaver in (d) were averaged for statistical analysis. (For interpretation of the references to colour in this figure legend, the reader is referred to the Web version of this article.)

contralateral eyes of the same animal, the average values were Q(P→0) = 4.0 [−2.2, 10.3] nl/min ($p > 0.05$, N = 5 mice) with P(P→0) = 0.00 [−0.05, 0.06] mmHg ($p > 0.05$, N = 5). We therefore measured pressure-independent flows that were indistinguishably different from zero, both soon after cannulation and after multi-pressure perfusion. Thus, in our hands, it appears that there is zero or no significant pressure-independent flow in post-mortem cadaveric eyes.

3.2. Effect of humidity on evaporation and pressure-independent flow

The effect of humidity on pressure-independent flow was assessed in Group 2 by measuring Q at P = 0 at high humidity, and then decreasing the relative humidity to room levels whilst continuing to monitor Q at P = 0. At high RH, the pressure-independent flow rate was insignificantly different from zero (Fig. 4a). As the humidity was decreased, however, the measured flow rate passing through the perfusion system, and hence the net pressure-independent flow leaving the eye, increased. The system was then left at room humidity, and the non-zero flow rate persisted for an hour (Fig. 4a). The difference between values of Q at P = 0 at high and low humidity measured in four eyes from three mice is shown in Fig. 4b. Q at P = 0 increased in all eyes by 20–60 nl/min, despite a drop of DBG remaining on the corneal surface throughout the measurement. These data demonstrate that evaporative losses driven by relatively low room humidity, even in the presence of a hydrated cornea, may contribute to pressure-independent flows. Importantly, evaporative driven flows represent a significant fraction of previously reported values of aqueous humour inflow (Toris et al., 2016; Millar et al., 2011) and pressure-independent outflow (Millar et al., 2011, 2015; Yu et al., 2020).

3.3. Postmortem facility and non-linearity

Group 2 (cannulation with postmortem delay) had an average outflow facility (C_r at P_r = 8 mmHg) of 4.3 [3.9, 4.8] nl/min/mmHg (N = 10), while Group 3 (cannulation without postmortem delay) had an average outflow facility of 4.0 [3.6, 4.4] nl/min/mmHg (N = 12) (Fig. 5a and b). The effect of postmortem delay before cannulation therefore did not appear to alter outflow facility between the two groups ($p > 0.05$).

As demonstrated in Fig. 2c, the flow-pressure relationship was non-linear (as following Section 3.1, it must pass through zero). This non-linearity, represented by β, is shown in Fig. 5c and d for Groups 2 and 3, respectively. Group 2 had a mean β of 0.09 [−0.10, 0.28] (N = 10), which was not statistically different from zero ($p > 0.05$). Group 3 however, had a mean β of 0.51 [0.37, 0.65] (N = 12) that was statistically greater than zero ($p < 0.001$). Thus in general, the flow-pressure relationship may exhibit non-linearity in the cadaveric eye, but when a postmortem delay was allowed to occur prior to cannulation, the non-linearity of the flow-pressure relationship, represented by β, was significantly reduced ($p < 0.01$).

3.4. Comparison between ex vivo and postmortem facility measurements

In order to evaluate the differences between *ex vivo* and postmortem approaches, we compared the postmortem measurements of C_r and β (Equation (2)) from Groups 2 and 3 to comparable data from 43 *ex vivo* eyes that were perfused contemporaneously with eyes in the Groups 2 and 3 (Reina-Torres et al., 2019; Reina-Torres et al., 2020a).

The mean reference facility (Fig. 6a) of the *ex vivo* data (N = 43) was 4.3 [3.7, 4.8] nl/min/mmHg, which was not statistically different from either postmortem group as determined by a Kruskal-Wallis test ($p > 0.05$). The spread of data for *ex vivo* measurements was, however, much broader with a ±2 standard deviation range of 1.8–9.9 nl/min/mmHg, as compared to 3.1–5.9 nl/min/mmHg and 2.8–5.6 nl/min/mmHg from Groups 2 and 3, respectively. This corresponds to a reduction in variability between eyes of ~65% in our postmortem measurements as compared to prior *ex vivo* measurements. The greater variability in the *ex vivo* group may be attributable in part to inter-cohort variability or

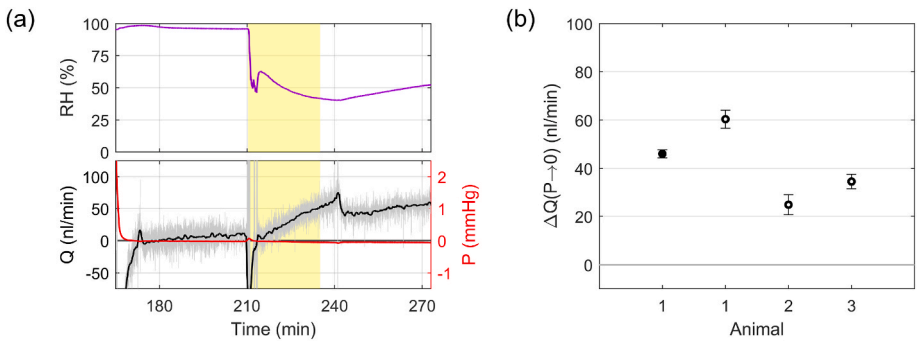

Fig. 4. The effect of humidity on pressure-independent flow measurements. a) Relative humidity (RH) in the humidity chamber, the flow rate (Q, grey with filtered signal in black) and the pressure (P, red). Yellow region indicates the time during which the air in the humidity chamber was exchanged with room air. b) The increase in flow rate at zero pressure between high and low humidity conditions, termed $\Delta Q(P = 0)$, for 4 eyes from 3 mice. Measurements from OS are indicated as hollow points. Ambient RH values were 52% for Animal 1, 24% for Animal 2 and 22% for Animal 3. (For interpretation of the references to colour in this figure legend, the reader is referred to the Web version of this article.)

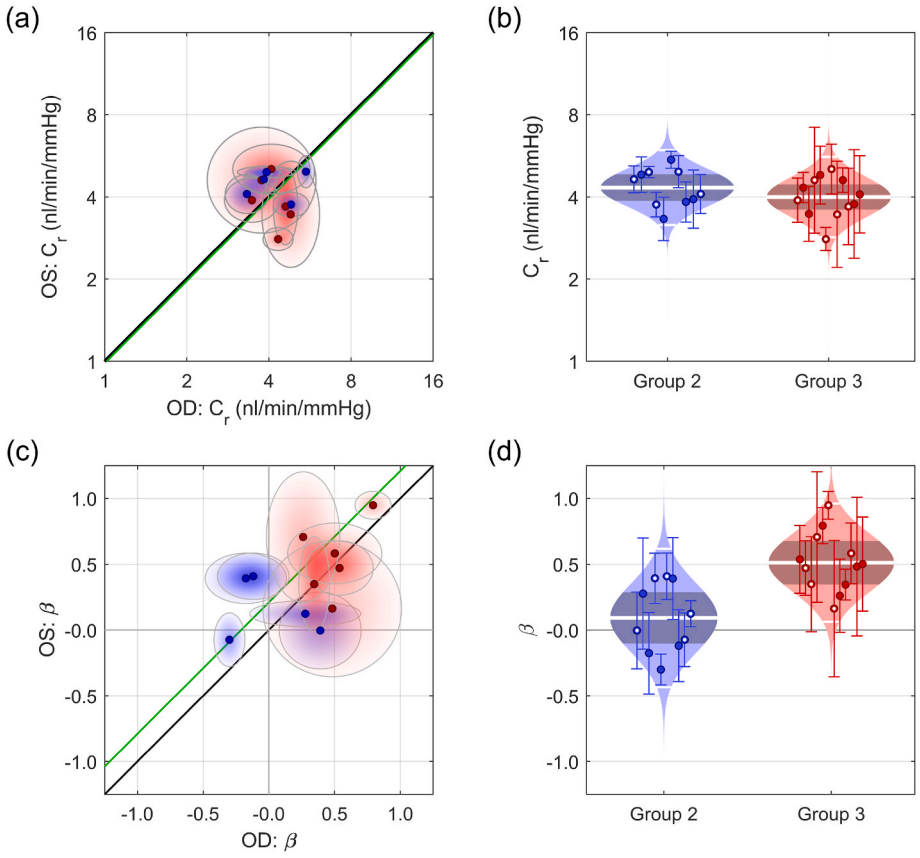

Fig. 5. Reference outflow facility and the non-linearity of the flow-pressure relationship in post-mortem mouse eyes. Data points in (a) and (c) represent the paired fit parameters of reference facility (C_r) and non-linearity (β) for both eyes from each mouse of Group 2 (blue – cannulation 40 min after euthanisation) and Group 3 (red – cannulation 15 min after euthanisation). Grey ellipses in panels (a) and (c) represent the 95% confidence interval on fitted values of C_r and β based on Eq. (2). In (a) and (c) the black line represents the line of unity while the green line shows the mean fold difference between contralateral eyes for both groups combined. In b) and d) data points show the fitted parameters of C_r (b) and β (d) with the CI on the fitted parameters given by the error bars, OS are marked by hollow data points. Shaded regions show best estimates of the sample distributions while dark bands show 95% CI on the mean values. Thin and thick white lines show the sample mean and two-standard deviations respectively. (For interpretation of the references to colour in this figure legend, the reader is referred to the Web version of this article.)

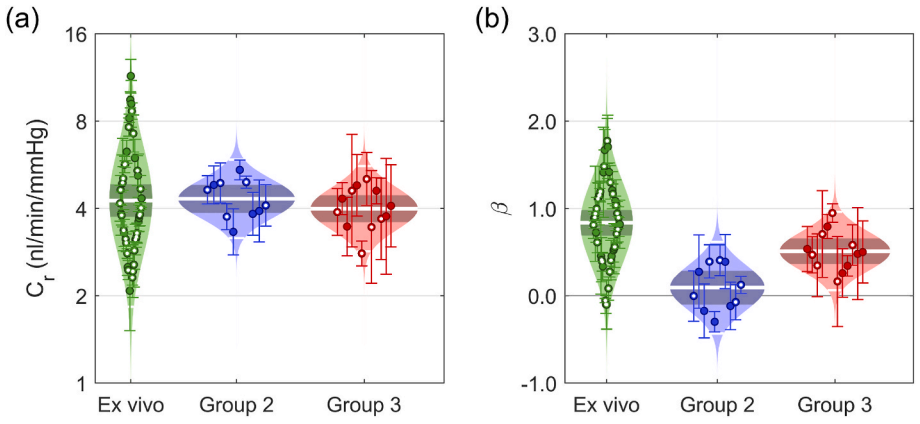

Fig. 6. Comparison of outflow facility and non-linearity parameters between postmortem perfusions (Groups 2 and 3) versus prior reports of *ex vivo* perfusions conducted contemporaneously with those in Groups 2 and 3. a) Data points show regression fit parameters of C_r (a) and β (b) with the 95% CI on the fitted parameters given by the error bars. In a) and b), shaded regions show best estimates of the sample distributions with dark central bands showing 95% CI on the mean values. Thick and thin white lines show the sample mean and two-sigma respectively. In all panels hollow data points mark measurements from left eyes.

seasonable variations in *in vivo* housing conditions, such as humidity, which can affect outflow facility measured after death (Reina-Torres et al., 2019).

The mean β of the *ex vivo* group was 0.84 [0.69, 0.98] (N = 43). The Kruskal-Wallis test rejected the null hypothesis that there were no differences between the groups ($p < 0.001$). Post-hoc analysis with Dunn's test did not detect a statistical difference in β between Group 3 and *ex vivo* ($p > 0.05$) or between Groups 2 and 3 ($p > 0.05$), but indicated a statistically lower β in Group 2 compared to *ex vivo* eyes ($p < 0.001$).

4. Discussion

4.1. Implications for outflow facility measurements in mice

Assumptions about the linearity of the flow-pressure relationship and the magnitude of pressure-independent outflow strongly influence how outflow facility is determined in all species and under all conditions. This is because outflow facility cannot be measured directly, but can only be determined by fitting a mathematical model to flow and pressure data measured during perfusion. The most common mathematical model assumes a linear flow-pressure relationship and allows for a non-zero intercept, which is typically interpreted as pressure-independent outflow (or sometimes explicitly referred to as uveoscleral outflow). Thus, assumptions about whether pressure-independent outflow exists (or not), as well as assumptions about the shape of the flow-pressure relationship, conspire to influence any determination of outflow facility (whether *ex vivo*, postmortem *in situ* or *in vivo*). Accurately assessing outflow facility thus requires validation of assumptions about the magnitude of pressure-independent outflow, as well as the shape of the flow-pressure relationship (linear or otherwise).

In our previous study of enucleated *ex vivo* mouse eyes submerged under isotonic saline, we showed that the pressure independent flow Q_0 was indistinguishably different from zero when IOP was set to 0 mmHg (Madekurozwa et al., 2017). Similarly, in this study, we showed that at both 30 min and 160 min after death, the value of Q_0 was insignificantly different from zero when the eyes were retained *in situ* and the cadaver was maintained within a high humidity environment. As inflow (Q_{in}) can be safely assumed to be zero after death and because we eliminated the driving force for evaporation, we demonstrated by direct measurement that the pressure-independent outflow is indistinguishably different from zero in C57BL/6J cadaveric mouse eyes. Having established this, we were able to show that the flow-pressure relationship in cadaveric mouse eyes may exhibit significant non-linearity. These findings support the use of Equation (2) to determine outflow facility, which assumes zero pressure-independent flow and allows for non-linearity in the form of a power-law (but which also can allow for linearity when $\beta = 0$). These findings challenge prior approaches using a linear fit with a free intercept to account for pressure-independent flow via extrapolation, as has been used to determine outflow facility in previous studies of postmortem mouse eyes (Lopez et al., 2017; Millar et al., 2011, 2015). The implications of these findings were demonstrated previously in *ex vivo* mouse eyes, in which inappropriate application of a linear model with a free intercept led to significant errors of several fold in estimates of outflow facility (Madekurozwa et al., 2017; Sherwood et al., 2016).

4.2. Postmortem studies provide insight regarding the mechanism of pressure-independent outflow

Although it is not possibly to discern flow through specific anatomical pathways via perfusion alone, pressure-independent outflow is typically interpreted as unconventional outflow. Physiologically, unconventional outflow comprises two pathways: osmotically driven flow into the choroid (uveovortex outflow) and pressure driven flow across the sclera from the suprachoroidal space (uveoscleral outflow) (Johnson et al., 2017). As uveoscleral outflow is pressure driven, uveoscleral outflow should not impose a non-zero pressure-independent flow at zero perfusion pressure. However, osmotically driven uveovortex flow could in principle occur in the absence of a hydrostatic pressure gradient to contribute to non-zero outflow at zero IOP.

In this study, we demonstrated that postmortem cadaveric eyes exhibit zero pressure-independent flow, or no pressure-independent outflow that is detectibly different from zero (assuming that aqueous humour secretion ceases postmortem). This implies that any uveovortex outflow is rapidly eliminated after death in cadaveric eyes. Presumably, any stationary blood remaining in the choroid would retain some osmotic/oncotic gradient necessary to drive pressure-independent outflow, but this gradient would likely decrease over time as aqueous humour enters the choroidal vasculature and dilutes the constituents that create the osmotic pressure gradient. Further, severing of the femoral vein/artery as done in this study would decrease systemic blood pressure, which combined with intraocular pressurisation would tend to eject blood from the choroidal vasculature. This may significantly reduce choroidal blood volume and thus reduce the osmotic driving force for pressure-independent outflow. Alternatively, as the choroid is largely composed of blood vessels, blood ejection from the choroid may cause the choroidal or suprachoroidal pathways to collapse, restricting the pathway for aqueous to access the choriocapillaris where resorption occurs (Bill, 1977). Thus, the loss of systemic blood pressure leading to collapse of the choroid may have contributed to the elimination of both uveoscleral and uveovortex outflow in the cadaveric mouse eye, resulting in zero measured flow rate at zero intraocular pressure. More research is needed to understand the factors regulating uveoscleral and uveovortex outflow.

In experiments of enucleated and postmortem eyes there is a progressive loss of corneal transparency with time after death, which maybe partially attributed to corneal swelling. In theory, it is possible that corneal swelling could affect the measured flow rate at zero pressure, which we attribute to pressure-independent outflow. Approximating the cornea as a spherical cap with a diameter of 3 mm, depth of 1 mm and thickness of 0.1 mm, predicts a corneal volume of approximately 1 μl. If the cornea swelled to twice its normal thickness over 30 min, then this would correspond to a flow rate from the anterior chamber of 33 nl/min, which is comparable to flow rates measured during perfusion. However, at zero pressure, we measure a flow rate that is indistinguishable from zero, both at ~75 min after death (Group 1) and at ~190 min after death (Group 2), suggesting that any swelling that occurs has a negligible effect on the measured flow rate. This may be because, as corneal swelling typically occurs by posterior displacement of the endothelial surface (Li et al., 2004), any volume of fluid in the anterior chamber that contributes to corneal swelling is replaced exactly by the volume of swollen cornea. In such a scenario, there is zero net fluid motion from the anterior chamber and therefore no effect of swelling on the measured flow rate.

4.3. The confounding effect of evaporation on the measurement of pressure-independent outflow

Although drops of PBS or other water-based solutions are often placed on the corneal surface to inhibit evaporation from the eye, evaporation still occurs from the fluid on the ocular surface. This loss of water will increase the osmolarity of the surface fluid and create an osmotic gradient that drives flow across the cornea from the anterior chamber independent of a pressure gradient. This phenomenon was originally described by Mishima and Maurice (1961a) to explain corneal swelling that occurs during lid closure in rabbits and the corneal thinning that occurs upon lid opening, which they related to evaporative changes in tear film osmolarity.

During lid opening, evaporation is minimised by the presence of the oily tear film layer produced by the Meibomian glands. Disruption of the oil layer increases evaporation by more than 10-fold, because the epithelium offers negligible resistance to evaporation (Mishima and

Maurice, 1961b). In rabbits, evaporation led to water loss from the anterior chamber, as determined by electrical conductivity measurements that showed an increase in aqueous humour salinity when eyelids were open relative to contralateral eyes where the eyelids were fixed closed (Mishima and Maurice, 1961a). Other authors have noted the importance of adequate ocular hydration in anaesthetised animals by observing and grading the severity of cataract formation that is driven by small changes in aqueous humour osmolarity (Ridder et al., 2002; Fraunfelder and Burns, 1970). Literature data thus demonstrate that evaporation from the ocular surface can drive water loss from the anterior chamber, which if left uncorrected would appear as a pressure-independent outflow.

In comparison to rabbits, the smaller mouse eye has a larger surface area relative to anterior chamber volume along with a thinner cornea, and thus the effects of evaporation are likely to be even more important in mice. In the current study, we investigated whether evaporation from the ocular surface could generate a detectible flow from the anterior chamber in mice. In a set of 4 eyes, reducing humidity from near saturation (RH>85%) to room levels led to an apparent pressure-independent outflow of 20–60 nl/min. This occurred even though drops of iso-osmotic saline were placed on the corneal surface at the start of the experiment to minimise osmotic effects. Comparing against a typical pressure-dependent outflow rate of 40 nl/min[3] in mice indicates that evaporation under standard room conditions has the potential to approximately double the measured flow rate. Importantly, this evaporative loss would manifest as a positive intercept on the pressure-flow relationship, regardless of the type of perfusion system used in the measurement (pressure or flow control[4]), which if left uncorrected could be interpreted as a pressure-independent outflow, as previously described (Boussommier-Calleja et al., 2015; Ficarrotta et al., 2018). Inadequate control of evaporation or humidity may explain why several previous studies of postmortem cadaveric mice reported non-zero values of pressure-independent outflow (Millar et al., 2011; Lopez et al., 2017; Aihara et al., 2002, 2003; Zhang et al., 2009; Yu et al., 2020).

We used a humidity chamber in the current study to minimise evaporation from the ocular surface. However, Zhang et al. (2002) developed an innovative approach to maintain a constant ocular surface osmolarity for *in vivo* perfusions, and thereby minimise artefactual osmotically driven outflow from the anterior chamber, without a humidity chamber (hence in the presence of evaporation). A saline drip was used to continuously replenish the ocular surface fluid at a rate of 10 μl/min with a nylon suture as a wick to prevent drop formation in wild-type CD1 mice. Importantly, they reported a zero infusion flow rate at spontaneous IOP, consistent with the absence of an evaporative effect expected under these conditions.

When evaporative losses are not prevented, the net loss of fluid from the eye results in an increase in the perceived value of Q_0. For instance, Mishima and Maurice (1961a) reported the average rate of fluid loss from the surface of a saline washed rabbit eye with an intact epithelium to be 47.6 μl/cm^2/hr when exposed to the air, as compared to 2.8 μl/cm^2/hr in eyes with a natural tear layer (owing to the oil layer secreted by the Meibomian glands). To estimate an equivalent value for C57BL/6J eyes, we assume the eye is a sphere of radius 1.7 mm (Li et al., 2014) and that evaporative losses only occur from the cornea which is approximately a third of the total surface area of the eye, as the rest of the eye is covered by hydrated tissue and muscle, evaporative losses from the sclera are not considered. Scaling down based on area yields an estimate of the total evaporative loss from the surface area of the eye without the oil layer of 90 nl/min which is comparable to the 20–60 nl/min reported in the current study, although we note that the magnitude would depend on stromal thickness and the exact value of room humidity. This estimate is also consistent with the measurements of Wisard et al. (2010), who measured the change in weight over time due to evaporation from enucleated eyes from C57BL/6J mice, from which we can estimate[5] a loss of 73 nl/min when evaporation was limited to one-third of the ocular surface. Thus, it seems likely that evaporation can account for most, if not all, of previously reported non-zero values of pressure-independent outflow in cadaveric mice. We therefore recommend that perfusion of *in situ* mouse eyes should be carried out within a humidity chamber to minimise evaporation or using the wick method of Zhang et al. (2002) to maintain ocular surface osmolarity.

4.4. Possible causes for the non-linearity of the flow-pressure relationship

The non-linearity of the flow-pressure relationship is represented by the parameter β in Equation (2), which can be interpreted as the constant of proportionality between relative changes in facility and relative changes in pressure. β was greater (meaning a larger relative change in facility per unit relative change in pressure) when eyes were cannulated soon after death in Group 3 versus after a postmortem delay in Group 2. Immediately after cannulation, fluid enters the eye from the perfusion system and pressurises the eye until intraocular pressure approximates the value of P_a set by the upstream reservoir. This pressurisation process may also drive posterior displacement of the iris and lens, known as anterior chamber (AC) deepening, as previously reported in mouse eyes (Boussommier-Calleja et al., 2015) and other species (Bárány, 1959) including humans (Ellingsen and Grant, 1971; Brubaker, 1975, Grant, 1963). AC deepening is likely enhanced if the eye is cannulated and pressurised from a low starting pressure or if there is little fluid in the posterior chamber to oppose posterior iridial displacement.

AC deepening increases outflow facility by applying inward-directed tension to the trabecular meshwork (Van Buskirk and Grant, 1973). Thus, it seems reasonable that AC deepening would be associated with a pressure-dependent increase in outflow facility, which would manifest as a positive value of β. Indeed, we suspect that AC deepening contributes to the positive β values often reported in enucleated mouse eyes (Reina-Torres et al., 2019; Madekurozwa et al., 2017, Reina-Torres et al., 2020b; Sherwood et al., 2016). Similar mechanisms should apply to cadaveric eyes, which may explain why the value of β was not statistically different between Group 3 and *ex vivo* eyes, although we suspect that the process of enucleation may enhance AC deepening and increase β by evacuating the posterior chamber. Regardless, the observation that β was approximately zero in Group 2 eyes (which had a longer postmortem delay prior to cannulation) was surprising, because the longer time between death and cannulation relative to Group 3 should have led to a lower starting IOP, which we expected would accentuate AC deepening and increase β. One potential explanation for this discrepancy is that rigor mortis or other postmortem changes may have stiffened the iridial muscles, such as the pupillary sphincter or iris dilator muscles. Stiffening of these muscles could have limited the extent

[3] Assuming a typical outflow facility of 5 nl/min/mmHg at physiological pressure drop of 8 mmHg between the anterior chamber and episcleral veins, yields 40 nl/min as an estimate of a typical conventional outflow rate in mice.

[4] For pressure based perfusion systems, the ocular volume remains constant at a given pressure. Hence the additional fluid leaving the eye due to evaporation would be replenished from the reservoir and increase the measured flow rate. For syringe pump based perfusion systems the flow from the perfusion system remains constant. Therefore, additional fluid leaving the eye due to evaporation would reduce the amount of fluid crossing the conventional outflow pathway and thereby decrease the measured intraocular pressure.

[5] Wisard et al. (2010) demonstrated evaporative loss from *ex vivo* C57BL/6J mouse eyes (N = 10) by measuring weight loss following enucleation, blotting the eye dry and exposing to room air (see Fig. 4 of Wisard et al., 2010). On average eyes lost 2.85 mg due to evaporation over a 13 min period. This leads to a total evaporative loss of 219 nl/min. Assuming that under cadaveric conditions, only one-third of the eye is exposed to room air and available for evaporation, these data predict an evaporative loss of 73 nl/min.

of AC deepening, potentially explaining the lower values of β in Group 3 eyes. Nonetheless, the similarity in C_r values between postmortem and *ex vivo* conditions, regardless of whether the eye was cannulated before or after a postmortem delay, suggests that the power-law model can yield robust estimates of the reference outflow facility that are relatively insensitive to factors contributing to the non-linearity in the Q-P relationship, such as AC deepening.

5. Conclusions

In the present study, we characterised and optimised the postmortem model for measuring outflow facility in C57BL/6J mouse eyes using *iPerfusion*. We showed significant similarities between *ex vivo* and postmortem eyes: both have similar values of outflow facility and no significant pressure-independent outflow. We demonstrated that evaporative losses, even when the eye was covered with a saline drop, can generate an artificial outflow comparable to conventional outflow, a mechanism that could explain previous reports of non-zero pressure independent flow in postmortem eyes. It is therefore critical that a humidity chamber or an alternative method of inhibiting osmotically driven flow across the cornea is used for postmortem, and likely *in vivo*, perfusions, lest an artefactual pressure-independent flow be recorded or interpreted.

Declaration of interest

JvBS and MM receive consultancy funding to provide *iPerfusion* systems.

Acknowledgements

This work was supported by an Imperial College London President's Scholarship. We acknowledge funding from the BrightFocus Foundation (G2015145) and National Eye Institute (EY022359). This project was supported by the Royal Academy of Engineering under the Research Fellowship Scheme (RF201617\16\18).

Appendix A. Supplementary data

Supplementary data to this article can be found online at https://doi.org/10.1016/j.exer.2022.109103.

References

Aihara, M., Lindsey, J.D., Weinreb, R.N., 2002. Reduction of intraocular pressure in mouse eyes treated with latanoprost. Investig. Ophthalmol. Vis. Sci. 43, 146–150.
Aihara, M., Lindsey, J.D., Weinreb, R.N., 2003. Aqueous humor dynamics in mice. Investig. Ophthalmol. Vis. Sci. 44, 5168–5173.
Akaishi, T., Odani-Kawabata, N., Ishida, N., Nakamura, M., 2009. Ocular hypotensive effects of anti-glaucoma agents in mice. J. Ocul. Pharmacol. Therapeut. 25, 401–408.
Bárány, E., 1959. On the mechanism by which chamber depth affects outflow resistance in excised eyes. Doc. Ophthalmol. 13, 84–89.
Bertrand, J.A., Schicht, M., Stamer, W.D., Baker, D., Sherwood, J.M., Lütjen-Drecoll, E., Selwood, D.L., Overby, D.R., 2020. The β4-subunit of the large-conductance potassium ion channel KCa1.1 regulates outflow facility in mice. Investig. Ophthalmol. Vis. Sci. 61, 41-41.
Bill, A., 1977. Basic physiology of the drainage of aqueous humor. Exp. Eye Res. 25, 291–304.
Boussommier-Calleja, A., Bertrand, J., Woodward, D.F., Ethier, C.R., Stamer, W.D., Overby, D.R., 2012. Pharmacologic manipulation of conventional outflow facility in ex vivo mouse eyes. Invest. Ophthalmol. Vis. Sci. 53, 5838–5845.
Boussommier-Calleja, A., Li, G., Wilson, A., Ziskind, T., Scinteie, O.E., Ashpole, N.E., Sherwood, J.M., Farsiu, S., Challa, P., Gonzalez, P., Downs, J.C., Ethier, C.R., Stamer, W.D., Overby, D.R., 2015. Physical factors affecting outflow facility measurements in mice. Invest. Ophthalmol. Vis. Sci. 56, 8331–8339.
Boussommier-Calleja, A., Overby, D.R., 2013. The influence of genetic background on conventional outflow facility in mice. Investig. Ophthalmol. Vis. Sci. 54, 8251–8258.
Brubaker, R.F., 1975. The effect of intraocular pressure on conventional outflow resistance in the enucleated human eye. Investig. Ophthalmol. Vis. Sci. 14, 286–292.
Camras, L.J., Sufficool, K.E., Camras, C.B., Fan, S., Liu, H., Toris, C.B., 2010. Duration of anesthesia affects intraocular pressure, but not outflow facility in mice. Curr. Eye Res. 35, 819–827.
Crowston, J.G., Aihara, M., Lindsey, J.D., Weinreb, R.N., 2004. Effect of latanoprost on outflow facility in the mouse. Invest. Ophthalmol. Vis. Sci. 45, 2240–2245.
Cumming, G., 2014. The new statistics: why and how. Psychol. Sci. 25, 7–29.
Ellingsen, B.A., Grant, W.M., 1971. The relationship of pressure and aqueous outflow in enucleated human eyes. Investig. Ophthalmol. Vis. Sci. 10, 430–437.
Ficarrotta, K.R., Bello, S.A., Mohamed, Y.H., Passaglia, C.L., 2018. Aqueous humor dynamics of the Brown-Norway rat. Investig. Ophthalmol. Vis. Sci. 59, 2529–2537.
Fraunfelder, F.T., Burns, R.P., 1970. Acute reversible lens opacity: caused by drugs, cold, anoxia, asphyxia, stress, death and dehydration. Exp. Eye Res. 10, 19–30.
Grant, W., 1963. Experimental aqueous perfusion in enucleated human eyes. Arch. Ophthalmol. 69, 783–801.
Grant, W.M., 1951. Clinical measurements of aqueous outflow. Am. J. Ophthalmol. 34, 1603–1605.
Heijl, A., Leske, M., Bengtsson, B., et al., 2002. Reduction of intraocular pressure and glaucoma progression: results from the early manifest glaucoma trial. Arch. Ophthalmol. 120, 1268–1279.
Johnson, M., Mclaren, J.W., Overby, D.R., 2017. Unconventional aqueous humor outflow: a review. Exp. Eye Res. 158, 94–111.
Kizhatil, K., Chlebowski, A., Tolman, N.G., Freeburg, N.F., Ryan, M.M., Shaw, N.N., Kokini, A.D.M., Marchant, J.K., John, S.W.M., 2016. An in vitro perfusion system to enhance outflow studies in mouse eyes. Investig. Ophthalmol. Vis. Sci. 57, 5207–5215.
Ko, M.K., Kim, E.K., Gonzalez JR., J.M., Tan, J.C., 2016. Dose- and time-dependent effects of actomyosin inhibition on live mouse outflow resistance and aqueous drainage tissues. Sci. Rep. 6, 21492.
Kwon, Y.H., Fingert, J.H., Kuehn, M.H., Alward, W.L.M., 2009. Primary open-angle glaucoma. N. Engl. J. Med. 360, 1113–1124.
Lei, Y., Overby, D.R., Boussommier-Calleja, A., Stamer, W.D., Ethier, C.R., 2011. Outflow physiology of the mouse eye: pressure dependence and washout. Investig. Ophthalmol. Vis. Sci. 52, 1865–1871.
Leske, M.C., Heijl, A., Hussein, M., Bengtsson, B., Hyman, L., Komaroff, E., 2003. Factors for glaucoma progression and the effect of treatment: the early manifest glaucoma trial. Arch. Ophthalmol. 121, 48–56.
Li, G., Farsiu, S., Chiu, S.J., Gonzalez, P., Lütjen-Drecoll, E., Overby, D.R., Stamer, W.D., 2014. Pilocarpine-induced dilation of schlemm's canal and prevention of lumen collapse at elevated intraocular pressures in living mice visualized by OCT. Investig. Ophthalmol. Vis. Sci. 55, 3737–3746.
Li, G., Lee, C., Agrahari, V., Wang, K., Navarro, I., Sherwood, J.M., Crews, K., Farsiu, S., Gonzalez, P., Lin, C.-W., Mitra, A.K., Ethier, C.R., Stamer, W.D., 2019. In vivo measurement of trabecular meshwork stiffness in a corticosteroid-induced ocular hypertensive mouse model. Proc. Natl. Acad. Sci. Unit. States Am. 116, 1714–1722.
Li, G., Schmitt, H., Johnson, W.M., Lee, C., Navarro, I., Cui, J., Fleming, T., Gomez-Caraballo, M., Elliott, M.H., Sherwood, J.M., Hauser, M.A., Farsiu, S., Ethier, C.R., Stamer, W.D., 2020. Integral role for lysyl oxidase-like-1 in conventional outflow tissue function and behavior. Faseb. J. 34, 10762–10777.
Li, L.Y., Tighe, B.J., Ruberti, J.W., 2004. Mathematical modelling of corneal swelling. Biomech. Model. Mechanobiol. 3, 114–123.
Lopez, N.N., Patel, G.C., Raychaudhuri, U., Aryal, S., Phan, T.N., Clark, A.F., Millar, J.C., 2017. Anterior chamber perfusion versus posterior chamber perfusion does not influence measurement of aqueous outflow facility in living mice by constant flow infusion. Exp. Eye Res. 164, 95–108.
Madekurozwa, M., Reina-Torres, E., Overby, D.R., Sherwood, J.M., 2017. Direct measurement of pressure-independent aqueous humour flow using iPerfusion. Exp. Eye Res. 162, 129–138.
Madekurozwa, M., Stamer, W.D., Reina-Torres, E., Sherwood, J.M., Overby, D.R., 2021. The ocular pulse decreases aqueous humour outflow resistance by stimulating nitric oxide production. Am. J. Physiol. Cell Physiol.
Millar, J.C., Clark, A.F., Pang, I.H., 2011. Assessment of aqueous humor dynamics in the mouse by a novel method of constant-flow infusion. Invest. Ophthalmol. Vis. Sci. 52, 685–694.
Millar, J.C., Phan, T.N., Pang, I.-H., Clark, A.F., 2015. Strain and age effects on aqueous humor dynamics in the mouse. Investig. Ophthalmol. Vis. Sci. 56, 5764–5776.
Mishima, S., Maurice, D.M., 1961a. The effect of normal evaporation on the eye. Exp. Eye Res. 1, 46–52.
Mishima, S., Maurice, D.M., 1961b. The oily layer of the tear film and evaporation from the corneal surface. Exp. Eye Res. 1, 39–45.
Morrison, J.C., Nylander, K.B., Lauer, A.K., Cepurna, W.O., Johnson, E., 1998. Glaucoma drops control intraocular pressure and protect optic nerves in a rat model of glaucoma. Investig. Ophthalmol. Vis. Sci. 39, 526–531.
Overby, D.R., Bertrand, J., Schicht, M., Paulsen, F., Stamer, W.D., Lütjen-Drecoll, E., 2014. The structure of the trabecular meshwork, its connections to the ciliary muscle, and the effect of pilocarpine on outflow facility in mice. Investig. Ophthalmol. Vis. Sci. 55, 3727–3736.
Quigley, H.A., Broman, A.T., 2006. The number of people with glaucoma worldwide in 2010 and 2020. Br. J. Ophthalmol. 90, 262–267.
Reina-Torres, E., Bertrand, J.A., O'callaghan, J., Sherwood, J.M., Humphries, P., Overby, D.R., 2019. Reduced humidity experienced by mice in vivo coincides with reduced outflow facility measured ex vivo. Exp. Eye Res. 186, 107745.
Reina-Torres, E., Boussommier-Calleja, A., Sherwood, J.M., Overby, D.R., 2020a. Aqueous humor outflow requires active cellular metabolism in mice. Invest. Ophthalmol. Vis. Sci. 61, 45.
Reina-Torres, E., De Ieso, M.L., Pasquale, L.R., Madekurozwa, M., Van Batenburg-Sherwood, J., Overby, D.R., Stamer, W.D., 2020b. The vital role for nitric oxide in intraocular pressure homeostasis. Prog. Retin. Eye Res., 100922
Reina-Torres, E., Wen, J.C., Liu, K.C., Li, G., Sherwood, J.M., Chang, J.Y.H., Challa, P., Flügel-Koch, C.M., Stamer, W.D., Allingham, R.R., Overby, D.R., 2017. VEGF as a

paracrine regulator of conventional outflow facility. Investig. Ophthalmol. Vis. Sci. 58, 1899–1908.
Ridder, W.H.I., Nusinowitz, S., Heckenlively, J.R., 2002. Causes of cataract development in anesthetized mice. Exp. Eye Res. 75, 365–370.
Rosner, B., 1982. Statistical methods in ophthalmology: an adjustment for the intraclass correlation between eyes. Biometrics 38, 105–114.
Roy Chowdhury, U., Rinkoski, T.A., Bahler, C.K., Millar, J.C., Bertrand, J.A., Holman, B. H., Sherwood, J.M., Overby, D.R., Stoltz, K.L., Dosa, P.I., Fautsch, M.P., 2017. Effect of Cromakalim Prodrug 1 (CKLP1) on aqueous humor dynamics and feasibility of combination therapy with existing ocular hypotensive agents. Investig. Ophthalmol. Vis. Sci. 58 (13), 5731–5742.
Sherwood, J.M., Reina-Torres, E., Bertrand, J.A., Rowe, B., Overby, D.R., 2016. Measurement of outflow facility using iPerfusion. PLoS One 11, e0150694.
Smith, R.S., 2002. Systematic Evaluation of the Mouse Eye: Anatomy, Pathology, and Biomethods. CRC Press, Boca Raton.
Stamer, W.D., Acott, T.S., 2012. Current understanding of conventional outflow dysfunction in glaucoma. Curr. Opin. Ophthalmol. 23, 135–143.
Toris, C.B., Fan, S., Johnson, T.V., Camras, L.J., Hays, C.L., Liu, H., Ishimoto, B.M., 2016. Aqueous flow measured by fluorophotometry in the mouse. Investig. Ophthalmol. Vis. Sci. 57, 3844–3852.
Van Buskirk, E.M., Grant, W.M., 1973. Lens depression and aqueous outflow in enucleated primate eyes. Am. J. Ophthalmol. 76, 632–640.
Whitlock, N.A., Mcknight, B., Corcoran, K.N., Rodriguez, L.A., Rice, D.S., 2010. Increased intraocular pressure in mice treated with dexamethasone. Invest. Ophthalmol. Vis. Sci. 51, 6496–6503.
Wisard, J., Chrenek, M.A., Wright, C., Dalal, N., Pardue, M.T., Boatright, J.H., Nickerson, J.M., 2010. Non-contact measurement of linear external dimensions of the mouse eye. J. Neurosci. Methods 187, 156–166.
Yelenskiy, A., Ko, M.K., Chu, E.R., Gonzalez, J.M., Siegmund, K., Tan, J.C., 2017. Total outflow facility in live C57BL/6 mice of different age. Biomed. Hub 2, 6-6.
Yu, L., Zheng, Y., Liu, B.J., Kang, M.H., Millar, J.C., Rhee, D.J., 2020. Secreted protein acidic and rich in cysteine (SPARC) knockout mice have greater outflow facility. PLoS One 15 e0241294-e0241294.
Zhang, D., Vetrivel, L., Verkman, A.S., 2002. Aquaporin deletion in mice reduces intraocular pressure and aqueous fluid production. J. Gen. Physiol. 119, 561–569.
Zhang, Y., Davidson, B.R., Stamer, W.D., Barton, J.K., Marmorstein, L.Y., Marmorstein, A.D., 2009. Enhanced inflow and outflow rates despite lower IOP in Bestrophin-2 deficient mice. Investig. Ophthalmol. Vis. Sci. 50, 765–770.